International Journal of Latest Engineering and Management Research (IJLEMR)
ISSN: 2455-4847
www.ijlemr.com || REETA-2K16 ǁ PP. 60-71

Coordination of Solar PV and Battery Storage System of a Three – Level NPC Inverter Using FLC

K.PRAVALLIKA[1] T.MADHURANTAKA [2]
[1](*EEE Department, SV College of Engineering, Tirupati, India)*
[2]*(EEE Department, SV College of Engineering, Tirupati, India)*

Abstract: In this paper, a novel configuration of a three level neutral-point-clamped (NPC) inverter that can integrate solar photovoltaic (PV) with battery storage in a grid-connected system is proposed. The energy of the proposed topology lies in a novel, lengthened unbalance three-level vector modulation technique that can engender the correct ac voltage under unbalanced dc voltage conditions. This paper presents the Fuzzy Logic controller design philosophy of the proposed configuration and the theoretical framework of the proposed modulation technique. An incipient Fuzzy Logic controller for the proposed system is additionally presented in order to control the power delivery between the solar PV, battery, and grid, which simultaneously provides extreme power point tracking (MPPT) operation for the solar PV. The efficacy of the proposed methodology is investigated by the simulation of several scenarios, including battery charging and discharging with different calibers of solar irradiation. The proposed methodology and topology is tested on MATLAB/SIMULINK Environment.
Key words: Battery storage, solar photovoltaic (PV), space vector modulation (SVM), three-level inverter.

I. INTRODUCTION

DUE to the world energy crisis and environmental quandaries caused by predictable power generation, renewable energy sources such as photovoltaic (PV) and wind generation systems are becoming more promising alternatives to supersede translation generation units for electricity generation [1], [2].Advanced power electronic systems are needed to utilize and develop renewable energy sources. In solar PV or wind energy applications, utilizing extreme power from the source is one of the most consequential functions of the potency electronic systems [3]–[5]. In three-phase applications, two types of power electronic configurations are commonly used to transfer power from the renewable energy resource to the grid: Single-stage and double-stage translation. In the Double-stage conversion for a PV system, the first stage is customarily a dc/dc converter and second stage is a dc/ac inverter. The function of the dc/dc converter is to facilitate the extreme power point tracking (MPPT) of the PV array and to engender the congruous dc voltage for the dc/ac inverter. The function of the inverter is to engender three-phase sinusoidal voltages or currents to transfer the potency to the grid in a grid-connected solar PV system or to the load in a stand-alone system [3]–[5].In the single-stage connection, only one converter is needed to consummate the double-stage functions, and hence the system will have a lower cost and higher efficiency, however, a more intricate control method will be required. The current norm of the industry for high power applications is a three-phase, single stage PV energy systems by utilizing a voltage-source converter (VSC) for power conversion [4].

One of the major concerns of solar and wind energy systems is their capricious and fluctuating nature. Grid-connected renewable energy systems accompanied by battery energy storage can surmount this concern. This withal can increment the flexibility of puissance system control and raise the overall availability of the system [2]. Translational, a converter is required to control the charging and discharging of the battery storage system and another converter is required for dc/ac power conversion; thus, a three phase PV system connected to battery storage will require two converters. This paper is concerned with the design and study of a grid-connected three-phase solar PV system integrated with battery storage utilizing only one three-level converter having the capability of MPPT and ac-side current control, and withal the ability of controlling the battery charging and discharging. This will result in lower cost, better efficiency and incremented springiness of puissance flow control.

The remnant of the paper is organized as follows. Section II describes the structure of a three-level inverter and associated capacitor voltages. Section III presents the proposed topology to integrate solar PV and battery storage and its associated control. Section IV describes the Fuzzy Logic Controller. Section V describes the simulation and validation of the proposed topology and associated control system. Section VI concludes the paper.

II. STRUCTURE OF A THREE-LEVEL INVERTER AND ITSCAPACITOR VOLTAGE CONSIDERATIONS

2.1 Three-Level Inverter

Since the introduction of three-level inverters in 1981 [6],[7], they have been widely used in several applications,

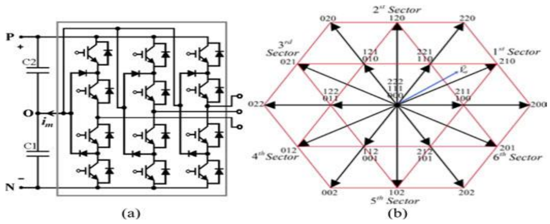

Fig.1. Typical three-level inverter (a) structure of circuit, and (b) three-level inverter space vector diagram for balanced dc-link capacitors [6].

Such as: motor drives, STATCOM, HVDC, pulse width modulation (PWM) rectifiers, active power filters (APFs), and renewable energy applications [7], [8]. Fig. 1(a) shows a typical three phase three-level neutral-point-clamped (NPC) inverter circuit topology. The converter has two capacitors in the dc side to produce the three-level ac-side phase voltages. Normally, the capacitor voltages are assumed to be balanced, since it has been reported that unbalance capacitor voltages can affect the ac side voltages and can produce unexpected behavior on system parameters such as even-harmonic injection and power ripple[7], [9]. Several papers have discussed methods of balancing these capacitor voltages in various applications [6], [7], [9]–[16].

2.2 Balanced Capacitors Voltage

Various strategies have been proposed to balance the capacitor voltages using modulation algorithms such as sinusoidal carrier based PWM (SPWM) or space vector pulse width modulation (SVPWM) [17]. In SPWM applications, most of the strategies are based on injecting the appropriate zero-sequence signal into the modulation signals to balance the dc-link capacitors [12], [13], [16], [18].In SVPWM applications, a better understanding of the things of the switching options on the capacitor voltages in the vector space has resulted in many strategies proposed to balance capacitors voltages in the three-level NPC inverter. These include capacitor balancing using translation SVPWM, virtual SVPWM (VSVPWM) and their combination [14], [15]. In vector control theory, ideally, the inverter must be able to generate the voltage output instantaneously, following the reference vector (*V*ref) generated by the control system. However, because of the limitation of the switches in the inverter, it is not possible to guarantee that any requested vector can be generated; as a matter of fact, only a limited number of vectors (27vectors for three-level inverter) can be generated. To overcome such difficulties, in any space vector modulation (SVM) scheme such as SVPWM and VSVPWM, the reference vector (*V*ref) is generated by selecting the appropriate available vectors in each time frame in such a way that the average of the applied vectors must be equal to the reference vector.

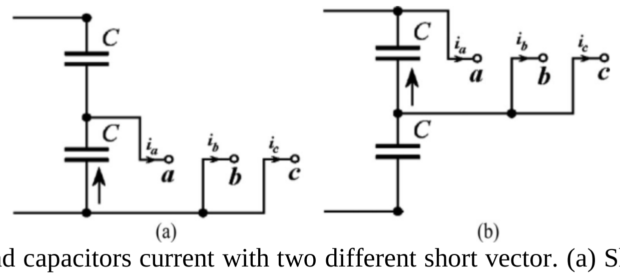

Fig.2. Equivalent circuit and capacitors current with two different short vector. (a) Short vector—100. (b) Short vector—211.

Equation (1) shows the mathematical relation between the timing of the applied vectors and the reference vector

$$\begin{cases} T_s \vec{V}_{\mathrm{ref}} = \sum_{i=1}^{n} T_i \vec{V}_i \\ T_s = \sum_{i=1}^{n} T_i \end{cases} \rightarrow (1)$$

Where *Ts* is the time frame and preferred to be as short as possible. It can be considered as a control update period where an average vector will be mathematically generated during this time duration. *Ti* is the corresponding time segment for selected inverter vector *VI* and *n* is the number of applied vectors. Generally, the reference vector is generated by three different vector (n = 3), and (1) can be converted to three different equation with three variables *T*1*, T2,* and *T*3 to be calculated. Several vector PWM techniques presented in [6, 7] [9]–[11], and [13]–[15] apply similar technique of timing calculation. Fig. 1(b) shows the space vector diagram of a three-level inverter for balanced dc-link capacitors [6]. It is made up of 27switching states, from which 19 different voltage vectors can be selected. The number associated with each vector in Fig.1 (b) represents the switching state of the inverter phases respectively. The voltage vectors can be categorized into five groups, in relation to their amplitudes and their things on different capacitor voltages from the view of the inverter ac side. They are six long vectors (200, 220, 020, 022, 002, and 202) three zero vectors(000, 111, and 222), six medium vectors (210 120 021 012 102 and 201) six upper short vectors (211 221 121 122 112and 212) and six lower short vectors (100, 110, 010, 011, 001,and 101).For generating V_{ref} , when one of the selections (*Vi*), is a short vector, then there are two choices that can be made which can produce exactly the same effect on the ac side of the inverter in the three wire connection (if voltages are balanced). For example, the short vector "211" will have the same effect as"100" on the ac side of the inverter. However, this choice will have different effect on the dc side, as it will cause a different dc capacitor to be chosen for the transfer of power from or to the ac side, and a different capacitor will be accused depending on the switching states and the direction of the ac side current. For example, Fig. 2 shows the connection of the capacitors when "100"or "211" is selected, demonstrating how different capacitors are involved in the transfer of power. Capacitor balancing in most reported three-level NPC inverter applications is achieved by the proper selection of the short vector.

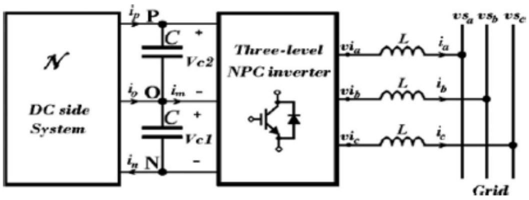

Fig.3. General Diagram of a grid connected three-wire three-level inverter.

In order to produce the ac-side waveform, the vector diagram of Fig. 1(b) is used, where the dc capacitor voltages are assumed to be balanced. Fig. 1(b) can then be used to determine the appropriate vectors to be selected and to calculate their corresponding timing (*Ti*) for implementing the required reference vector based on the expression given in (1). Although the control system is trying to ensure balanced capacitor voltages, should any unbalance occur during a transient or an unexpected operation, the above method will produce an inaccurate ac-side wave form which can be different from the actual requested vector by the control system. This can result in the production of even-harmonics; unbalanced current and unpredicted dynamic behavior. However, in some applications, the requirement of having balanced capacitor voltages may be too restrictive. It is possible to work with either balanced or unbalanced capacitor voltages. The method proposed in this paper is based on the freedom of having balance or unbalanced capacitor voltages. In such applications, it is important to be able to generate an accurate reference vector based on (1), irrespective of whether the capacitor voltages are balanced or not, to achieve the desired objectives of the system.

2.3 Unbalanced Capacitor Voltages

Fig. 3 shows a general structure of a grid-connected three level inverter presenting the dc and ac sides of the inverter. The dc-side system, shown as "*N*" can be made up of many circuit configurations, depending on the application of the inverter. For instance, the dc-side system can be a solar PV, a wind generator with a rectifying circuit, a battery storage system or a combination of these systems where the dc voltage across each capacitor can be different or equal. One of the main ideas of this paper is to have an overall view of the switching effect son a three-wire connection of a three-level NPC inverter with a combination of these systems on the dc side. Mathematically, in a three-wire connection of a two-level inverter, the *dq*o field, *vd, vq,* and *v*0 of the inverter in vector control can be considered as having two degrees of freedom in the control system; because the zero sequence voltage, *v*0 will have no effect on the system behavior in both the dc and the ac side of the inverter. However, in the three-level three-wire application illustrated in Fig. 3, with fixed *vd* and *vq* although *vo* will have no effect on the ac-side behavior, it can be useful to take advantage of *v*0 to provide a new degree of freedom to control the sharing of the capacitor voltages in the dc bus of the inverter. By doing this, it is now possible to operate and control the inverter under both balanced and unbalanced capacitor voltages.

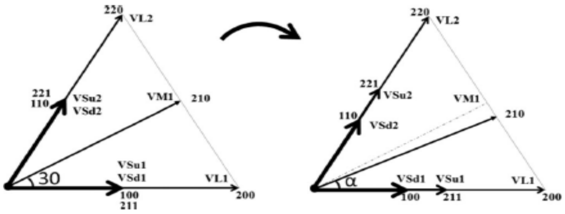

Fig.4.Vector diagram in the first sector of fig.(b) Presenting the change of the vectors using balanced dc and unbalanced dc assuming $Vc1 < Vc2$.

While continuing to generate correct the voltages in ac side. This feature is particularly useful in applications where the two capacitor voltages can be different, such as when connecting two PV modules with different MPPT points, or connecting a PV module across the two capacitors and including battery storage at the midpoint of the two capacitors, or connecting battery storage to each of the capacitors with the ability to transfer different power from each battery storage.

2.4 Effect of Unbalanced Capacitor Voltages on the Vector Diagram

In the vector diagram shown in Fig. 1(b), capacitor voltage unbalance causes the short and medium vectors to have different magnitudes and angles compared to the case when the capacitor voltages are balanced. Fig. 4 shows the differences between two cases as highlighted in the first sector of the sextant in Fig. 1(b) for $VC1 < VC2$. Vector related to the switching state _*VI* can be calculated as follows [20]:

$$\vec{V}_I = \frac{2}{3}\left(V_{aN} + \vec{a}V_{bN} + \vec{a}^2 V_{cN}\right) \qquad (2)$$

Where *a*= *ej* (2*π*3) and V_{aN} , V_{bN} and V_{cN} are the voltage values of each phase with reference to "*N*" in Fig. 1(a). Assuming that the length of the long vectors ($(2/3)V_{dc}$) is 1 unit and the voltage of capacitor *C*1, $V_{c1} = hV_{dc}$, for $0 \le h \le 1$, then the vectors in the first sector can be calculated using (2) and the results are given in (3)–(9)

$$\vec{V}sd1 = h \qquad (3)$$

$$\vec{V}su1 = 1 - h \qquad (4)$$

$$\vec{V}l1 = 1 \qquad (5)$$

$$\vec{V}l2 = \frac{1}{2} + \frac{\sqrt{3}}{2}j \qquad (6)$$

$$\vec{V}sd2 = h\left(\frac{1}{2} + \frac{\sqrt{3}}{2}j\right) \qquad (7)$$

$$\vec{V}su2 = (1-h)\left(\frac{1}{2} + \frac{\sqrt{3}}{2}j\right) \qquad (8)$$

$$\vec{V}m1 = \left(1 - \frac{h}{2}\right) + h\frac{\sqrt{3}}{2}j. \qquad (9)$$

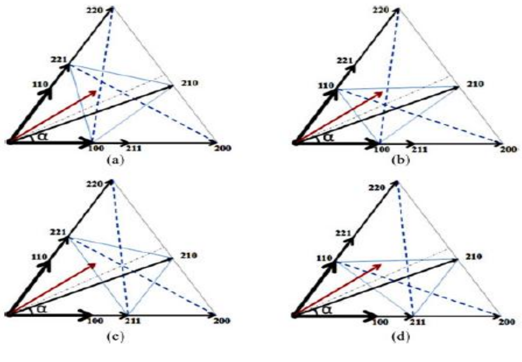

Fig.5. Different possible vector selection ideas

The vectors in the other sectors can be calculated similarly. Equations (3)–(9) show that the magnitudes and the angles of the vectors can change depending on the value of the capacitor voltages. For example, when $h = 0.5$, then the two capacitor voltages are the same and the two short vectors are the same, $Vsl1=Vsu1$. However, when the two capacitor voltages are different, the vectors will have different magnitudes. Since the short vectors are now different in magnitude, the choice of these short vectors will now have a different effect on both the dc and ac side. Traditionally, each pair of short vectors is considered to be redundant, as the selection of any of the short vectors at any instance will have the same effect on the ac side. However, when the two capacitor voltages are different, the short vectors cannot be considered to be redundant any more. Thus, when h=0.5, each different short vector needs different timing to generate the requested vector based on (1).

2.5 Selecting Vectors under Unbalanced DC Voltage Condition and Their Things on the AC Side of Inverter

To generate a reference vector based on (1), different combinations can be implemented. Fig. 5 shows different possible vector selections to generate a reference vector (V) in the first sector based on the selections of different short vectors. For example, to generate _V based on Fig. 5(a), one of following combinations can be selected with proper timing based on (1).The combinations are: (221–210–100), (221–220–100), (221–200–100), (221–200–Zero), (000–220–Zero), (220–200–Zero),where “Zero” can be “000” or “111” or “222”. This demonstrates that there is flexibility in choosing the correct vector selections. Although all of these selections with suitable timing can generate the same reference vector, they have different impact on the dc and ac side of the inverter in their instantaneous behavior. To investigate the ac-side behavior, the accuracy of the generated voltage must be examined.

As far as the ac side is concerned, ideally the requested voltage (t) should be exactly and simultaneously generated in the three phases of the inverter to have the correct instantaneous current in the ac side of the system. However, because of the limitation of the inverter to generate the exact value of the requested voltage in each phase, in the short time Ts, only the average value of the requested vector _V for the specified time window of Ts can be produced. To investigate the continuous time behavior of the ac-side voltages, the error vector _e (t) can be calculated in order to determine how far the generated voltage deviates from the requested vector as follows:

$$\vec{e}(t) = \vec{V}^{*}(t) - \vec{V}_{\mathrm{apl}}(t) \qquad (10)$$

$$E(t) \triangleq \left| \int_0^t \vec{e}(t)dt \right|; \qquad 0 \le t \le T_s \qquad (11)$$

Where Vapl(t) is the applied vector at the time “t”. This error can result in harmonic current across the impedance connected between the inverter and the grid. If this impedance is an inductor then the ripple in the inductors current IrL can be expressed as

$$\vec{I}r_L = 1/L \int_0^t \vec{e}(t)dt \qquad (12)$$

Where _e (t) is defined as

$$\vec{e}(t) \triangleq L\frac{d\vec{I}r_L}{dt}. \qquad (13)$$

To derive (13), it is assumed that the requested vector $V*(t)$ will generate sinusoidal current in the inductor, which is normally acceptable in the continuous time behavior of the system. Based on (11) and (12), the absolute value of error $E(t)$ is straight related to the magnitude of the inductors current ripple. Although based on (1) and (11), $E(Ts) = 0$ or the sum of errors during the period Ts is zero; but to diminish the magnitude of high frequency ripples, it is important to minimize the error at each time instant. To achieve this, the three nearest vectors (TNV) are usually used. For example, in Fig. 5(a), to generate the requested vector _$V*$, in the TNV method, the group (221,210, 100, or 211) appears to be the best three nearest vectors to be chosen. Also, to diminish $E(t)$, a smart timing algorithm for each vector in the TNV method has been proposed, such as dividing the time to apply each vector into two or more shorter times. However, this will have the effect of increasing switching losses. Dividing by two is common, acceptable solution. Moreover, reducing Ts will diminish the error $E(t)$ while improving the accuracy of the requested vector generated by the control system. According to the basic rule of digital control, accuracy of the requested vector calculation can be improved by reduction of the sampling time and the vector calculation time.

2.6 Selecting Vectors under Unbalanced DC Voltage Conditions and Their Things on DC Side of the Inverter

As far as the dc side is concerned, different vectors have different things on the capacitor voltages which depend on the sum of the incoming currents from the dc side and the inverter side. Fig. 3 shows *ip, io* , and *in* as dc-side system currents which are dependent on the dc-side system circuit topology and capacitor voltages. The currents coming from the inverter are related to the inverter switching and the ac side of inverter currents which can be straight affected by the implemented vectors in the inverter. Selecting different vectors will transfer ac-side currents and power differently to the capacitors as discussed in Section II-B. The instantaneous power transmitted to the dc side of the inverter from the ac side can be calculated as follows:

$$p(t) = v_{Ia}.i_a + v_{Ib}.i_b + v_{Ic}.i_c \qquad (14)$$

Where *vIa*, *vIb*, and *vIc* are the ac-side inverter instantaneous voltages with reference to the "*N*" point, and *ia, ib, ic* are inverter currents. For example, in the first sector of the vector diagram presenting Fig. 4, *p* (*t*) for the short vectors can be expressed by the following equations:

$$\begin{cases} p_{211}(t) = (1-h)\,Vdc * i_a \\ p_{100}(t) = hVdc * (-i_a) \end{cases} \qquad (15)$$

$$\begin{cases} p_{221}(t) = (1-h)\,Vdc * (-i_c) \\ p_{110}(t) = hVdc * i_c. \end{cases} \qquad (16)$$

Ignoring the dc-side system behavior, selecting the upper short vectors, "211" and "221," will affect the upper capacitor voltage, and selecting the lower short vectors, "100" and"110," will affect the lower capacitor voltage. For example, when *ia* >0, if vector "211" is selected, it will charge the upper capacitor without any effect on the lower capacitor voltage and if vector 100 is selected, it will discharge the lower capacitor without having any effect on the upper capacitor voltage. Busing (15) and (16), the rate of charging and discharging and their dependency on *h* and *Vdc* values and inverter currents can also be observed. However, for accurate investigations, the dc side system behavior needs to be considered in the control of charging and discharging rates of the capacitor voltages.

III. PROPOSED TOPOLOGY TO INTEGRATE SOLAR PV ANDBATTERY STORAGE AND ITS ASSOCIATED CONTROL

3.1 Proposed Topology to Integrate Solar PV and Battery Storage Using an Improved Unbalanced DC Functionality of a Three-Level Inverter

Based on the discussions in Sections I and II, two new configurations of a three-level inverter to integrate battery storage and solar PV shown in Fig. 6 are proposed, where no extra converter is required to connect the battery storage to the grid connected PV system. These can diminish the cost and improve the overall efficiency of the whole system particularly for medium and high power applications.

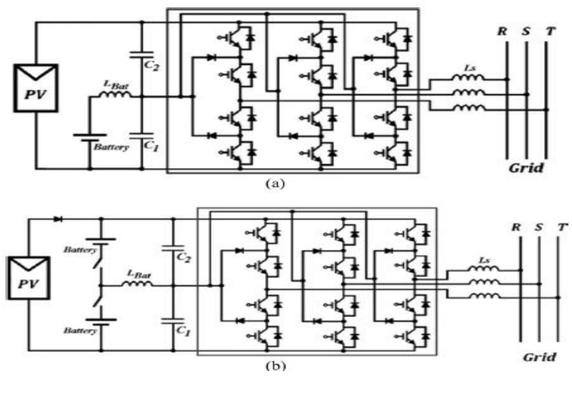

Fig.6. Proposed configurations for integrating solar PV and battery storage: (a) basic configuration; (b) improved configuration.

Fig. 6(a) shows the diagram of the basic configuration. In the proposed system, power can be transferred to the grid from the renewable energy source while allowing charging and discharging of the battery storage system as requested by the control system. The proposed system will be able to control the sum of the capacitor voltages ($VC1 + VC2 = Vdc$) to achieve the MPPT condition and at the same time will be able to control independently the lower capacitor voltage ($VC1$) that can be used to control the charging and discharging of the battery storage system. Further, the output of the inverter can still have the correct voltage waveform with low total harmonic distortion (THD) current in the ac side even under unbalanced capacitor voltage sin the dc side of the inverter. Although this configuration can operate under most conditions, however when the solar PV does not produce any power, the system cannot work properly with just one battery. Fig. 6(b) shows the improved configuration where two batteries are now connected across two capacitors through two relays. When one of the relays is closed and the other relay is open, the configuration in Fig. 6(b) is similar to that in Fig. 6(a) which can charge or discharge the battery storage while the renewable energy source can generate power. However, when the renewable energy is unavailable, both relays can be closed allowing the dc bus to transfer or absorb active and reactive power to or from the grid. It should be noted that these relays are selected to be ON or OFF as required; there is no PWM control requirement. This also provides flexibility in managing which of the two batteries is to be accused when power is available from the renewable energy source or from the grid. When one of the batteries is fully accused, the relay connected to this battery can be opened while closing the relay on the other battery to charge. Special consideration needs to be made to ensure that current through the inductor L_{batt} must be zero prior to opening any of these relays to avoid disrupting the inductor current and also to avoid damaging the relay.

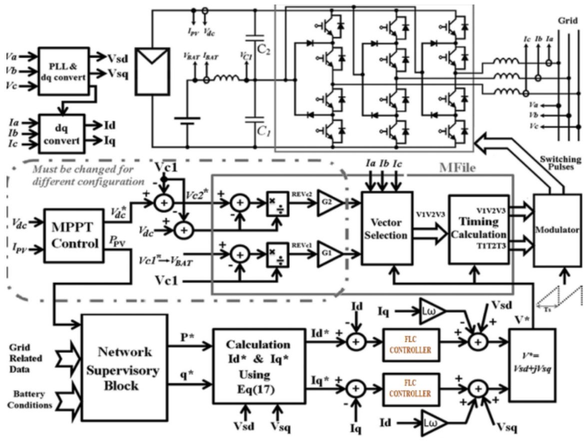

Fig.7. Control system diagram to integrate PV and battery storage

IV. FUZZY LOGIC CONTROLLER

Fuzzy logic uses fuzzy set theory, in which a variable is member of one or more sets, with a specified degree of membership. Fuzzy logic allow us to emulate the human reasoning process in computers, quantify imprecise information, make decision based on vague and in complete data, yet by applying a “defuzzification” process, arrive at definite conclusions.

The FLC mainly consists of three blocks

- Fuzzification
- Inference
- Defuzzification

RULES:

If input is NEGATIVE then output is POSITIVE
If input is ZERO then output is ZERO
If input is POSITIVE then output is NEGATIVE

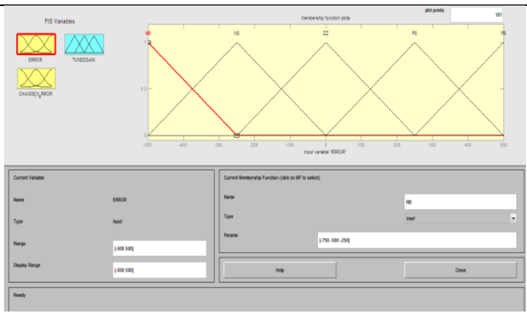

Fig..8 Fuzzy Inputs and Outputs

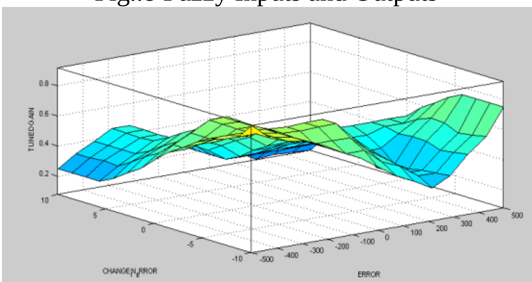

Fig.9 Surface of the Fuzzy logic controller

V. SIMULATION AND VALIDATION OF THE PROPOSEDTOPOLOGY AND CONTROL SYSTEM

Simulations have been carried out using MATLAB/Simulink to verify the effectiveness of the proposed topology and control system. An *LCL* filter is used to connect the inverter to the grid .Fig. 8 shows the block diagram of the simulated system.

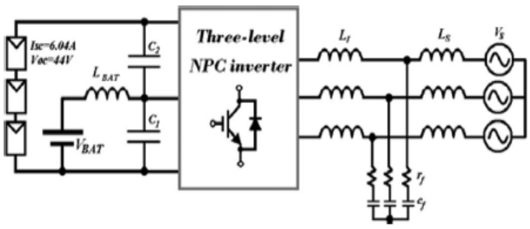

Fig. 8. Block diagram of the simulated system.

TABLE I
PARAMETERS OF THE SIMULATED SYSTEM

V_{BAT}	Vs (line)	L_{BAT}	C_1,C_2	L_f	L_s
60 V	50 V	5 mH	1000 uF	500 uH	900 uH
r_f	C_f	K_p	K_i	G_1	G_2
3 Ω	14 uF	2.9	1700	1	200

Three, series-connected PV modules are used in the simulation. The mathematical model of each of the PV units is given in (21) [21] and used in the simulation where *ISC* is the short circuit current of the PV. In the simulation, it is assumed that *ISC* will change with different irradiances. With a solar irradiation of 1000 W/m2, *ISC* is equal to 6.04A and the open circuit voltage of the PV panels will be equal to *VoC*= 44V. The main parameters of the simulated system are given in Table I.As discussed in Section III-B, *G*2 must be much more than*G*1 in order to achieve the MPPT condition and to have the flexibility to charge and discharge of the battery. Based on our experiments, any value more than 100 is suitable for this ratio. On the other hand, because the ratio of *G*2 /*G*1 will only affect the short-vector selection, increasing this ratio will not affect other results. This value has been selected to be 200 to have good control on *Vdc*, as shown in Table I. The role of *L*BAT is to smooth the battery current, especially in the transient condition. A wide range of values are acceptable for the inductor value, however, decreasing its value will increase the current overshoot of the battery. Also, its value is dependent of its adjacent capacitor value and its transient voltages. Due to the practical considerations (such as size and cost), the value of *L*BAT is preferred to be low and has been chosen to be 5 mH based our simulation studies. The values of *Kp* and *Ki* are selected by modeling the system in the *dq*-frame. The current control loop can be converted to a simple system after using the decoupling technique shown in Fig 7. The details of this method can be found in [22].For theoretical purposes, two different scenarios have been simulated to investigate the effectiveness of the proposed topology and the control algorithm using a step change in the reference inputs under the following conditions:

1) The effect of a step change in the requested active underactive power to be transferred to the grid when the solar irradiance is assumed to be constant.

2) The effect of a step change of the solar irradiation when the requested active and reactive power to be transmitted to the grid is assumed to be constant. In a practical system, a slope controlled change in the reference input is usually used rather than a step change to diminish the risk of mathematical internal calculation errors when working with a limited precision microprocessor system and also to prevent the protection system activation. Furthermore, in practical situations, the inputs of the systems normally do not change instantaneously as a step change, such as the sun irradiation. With this practical application in mind, the proposed system is simulated using a slope controlled change in the requested active power to be transferred to the grid when the solar irradiance is assumed to be constant

A. First Theoretical Scenario

In the first scenario, it is assumed that the solar irradiation will produce *ISC* = 5.61 A in the PV module according to (21). The MPPT control block, shown in Fig. 7, determines the requested PV module voltage *V∗dc* , which is 117.3 V to achieve the extreme power from the PV system that can generate558 W of electrical power. The requested active power to be transmitted to the grid is initially set at 662Wand is changed to 445Wat time *t* = 40 ms and the reactive power changes from zero to 250VAr at time *t* = 100ms.Fig. 9 show the results of the first scenario simulation. Fig. 9(a) and (b) shows that the proposed control system has correctly followed the requested active and reactive power, and Fig. 9(c) shows that the PV voltage has been controlled accurately (to be 177.3 V) to obtain the extreme power from the module. Fig. 9(d) shows that battery is discharging when the grid power is more than the PV power, and it is charging when the PV power is more than the grid power. Fig. 9(d) shows that before time *t* = 40 ms, the battery discharges at1.8 A since the power generated by the PV is insufficient. Aftertime *t* = 40 ms, the battery current is about –1.8 A, signifying that the battery is being accused from the extra power of the PV module. Fig. 9(e) shows the inverter ac-side currents, and Fig. 9(f) shows the grid-side currents with a THD less than1.29% due to the *LCL* filter. The simulation results in Fig.9show that the whole system produces a very good dynamic response.

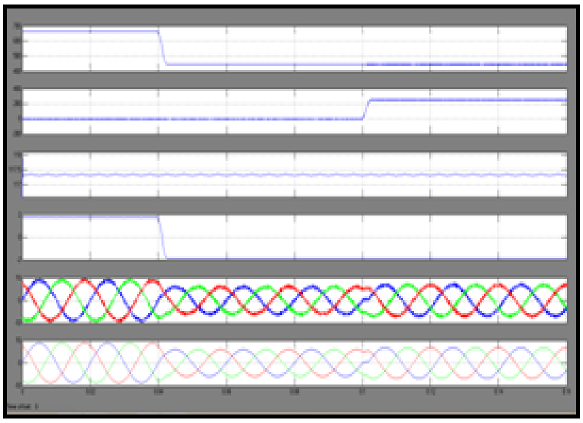

Fig.9.Simulated results for the first scenario. (a) Active power injected to the grid. (b) Reactive power injected to the grid. (c) PV module DC voltage. (d) Battery current. (e) Inverter AC current. (f) Grid current.

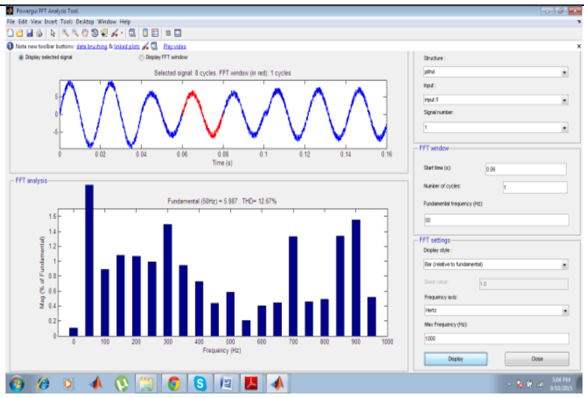

(a)

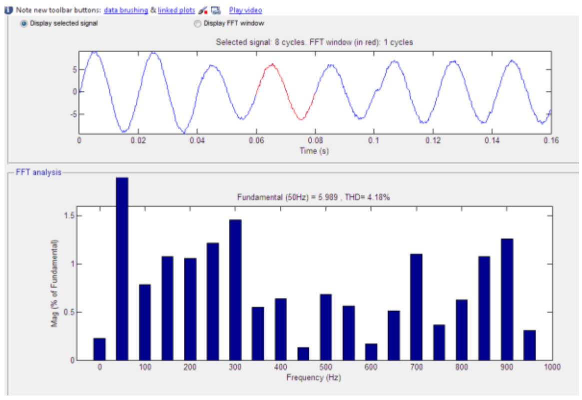

(b)

Fig 9.1 Total Harmonic Distortion of the Three Level NPC Output Current (a) Using PI Controller (b) Using Fuzzy Logic controller

Figure 9.1 show that Fuzzy Logic controller can achieve the less THD Values (4.18%) when compared with normal PI Controller (i.e.12.42%).

B. Second Theoretical Scenario

In the second scenario, it is assumed that the solar irradiation will change such that the PV module will produce *ISC*= 4.8, 4, and 5.61 A. The MPPT control block determines that *Vdc* needs to be 115.6, 114.1, and 117.3 V to achieve the extreme power from the PV units which can generate 485, 404, and 558 W, respectively. The requested active power to be transmitted to the grid is set at a constant 480 W and the reactive power is set to zero during the simulation time. Fig. 11 shows the results of the second scenario simulation. Fig.11(a) shows that the inverter is able to generate the requested active power. Fig. 11(b) shows that the PV voltage was controlled accurately for different solar irradiation values to obtain the relevant extreme power from the PV modules. Fig. 11(c) shows that the charging and discharging of the battery are correctly performed. The battery has supplemented the PV power generation to meet the requested demand by the grid. Fig. 11(d) illustrates that the quality of the waveforms of the grid-side currents are acceptable, which signifies that the correct PWM vectors are generated by the proposed control strategy.

By using the proposed strategy, the inverter is able to provide a fast transient response. Fig. 11(e) shows the *a*-phase voltage and current of the grid, which are always in-phase signifying that the reactive power is zero at all times.

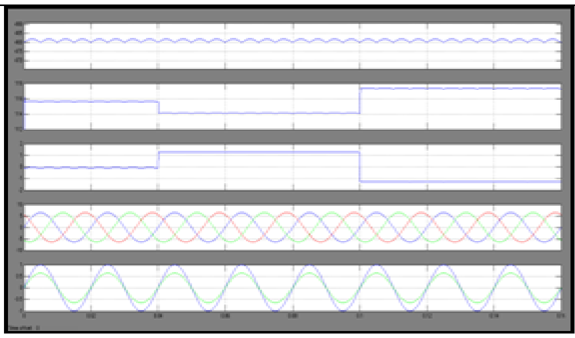

Fig.11.Simulated results for the second scenario. (a) Active power injected to the grid. (b) PV module DC voltage. (c) Battery currents. (d) Grid side currents. (e) Grid side Phase.

C. Practically Oriented Simulation

In the third simulation, the requested active power to be transmitted to the grid is initially set at 295Wand, at time t = 40ms, the requested active power starts to diminish as a slope controlled change and is finally stays constant at 165 W at t = 90 ms. It is assumed that the solar irradiation will produce *ISC*= 2.89 A in the PV module according to (21). The requested PV module voltage *Vdc* , to achieve MPPT condition will be 112.8 V to generate 305 W of electrical power. Fig. 12(a) shows that the active power transmitted to the grid diminishes and follows the requested active power. Fig. 12(b) shows the battery current which is about 0.1 A before t = 40 ms and then because of the diminished power transmission to the grid with constant PV output, the battery charging current is increased and finally fixed at about 2.2A. Fig. 12(c) shows the ac inverter currents slowly decreasing starting from 3.4*A*rms at t = 40 ms and finally stays constant at 1.9*A*rms at t = 90 Ms. During this simulation, the dc voltage is held at 112.8 Vto fulfill the MPPT requirement. It is important to note that during the simulations, the dc bus is working under unbalanced condition because the battery voltage during the simulation is equal to 60 V, and therefore, this particular scenario will not allow equal capacitor voltages.

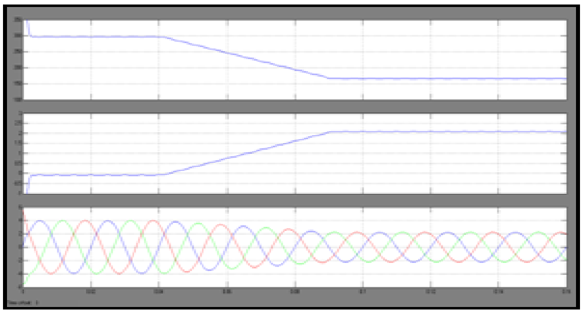

Fig.12. Simulated result for third scenario. (a) Active power injected to the grid. (b) Battery current. (c) Grid side currents.

VI. CONCLUSION

A three-level NPC voltage source inverter that can integrate both renewable energy and battery storage on the dc side of the inverter has been presented. A theoretical framework of a novel extended unbalance three-level vector modulation technique and Fuzzy Logic controller that can generate the correct ac voltage under unbalanced dc voltage conditions has been proposed. The proposed system has also been extant in order to control the power flow between solar PV, battery, and grid connected systems, and simultaneously MPPT operation is performed. The effectiveness of the proposed topology was tested using MATLAB/SIMULINK and results are presented. The MATLAB results demonstrate that the proposed system is able to control ac-side current, and battery charging and discharging currents at different levels of solar irradiation. The Proposed Fuzzy Logic control Strategy concludes that, the THD value for all inverter AC currents decreases from 12.42% to 4.18%.This will result in lower cost, better efficiency and increased flexibility of power flow control.

REFERENCES

[1]. O. M. Toledo, D. O. Filho, and A. S. A. C. Diniz "Distributed photovoltaic generation and energy storage systems: A review," *Renewable Sustainable Energy Rev* vol. 14, no. 1, pp. 506–511, 2010.

[2]. M. Bragard, N. Soltau, S. Thomas, and R. W. De Doncker, "The balance of renewable sources and user demands in grids: Power electronics for modular battery energy storage systems, *IEEE Trans. Power Electron.*, vol. 25, no. 12, pp. 3049–3056, Dec. 2010.

[3]. A. Yazdani and P. P. Dash, A control methodology and characterizationof dynamics for a photovoltaic (PV) system interfaced with a distributionnetwork, *IEEE Trans. Power Del.*, vol. 24, no. 3, pp. 1538–1551, Jul.2009.

[4]. A. Yazdani, A. R. Di Fazio, H. Ghoddami M. Russo, M. Kazerani, J.Jatskevich, K. Strunz, S. Leva, and J. A. Martinez, "Modeling guidelinesand a benchmark for power system simulation studies of three-phasesingle-stage photovoltaic systems," *IEEE Trans Power Del.*, vol. 26 no. 2,pp. 1247–1264, Apr. 2011.

[5]. M. A. Abdullah, A. H. M. Yatim, C. W. Tan, and R. Saidur "A reviewof extreme power point tracking algorithms for wind energy systems,"*Renewable Sustainable Energy Rev.*, vol. 16, no.5, pp. 3220–3227, Jun.2012.

[6]. S. Burusteta, J. Pou, S. Ceballos, I. Marino, and J. A. Alzola, "Capacitor voltage balance limits in a multilevel-converter-based energy storage system," in *Proc. 14th Eur Conf. Power Electron. Appl.*, Aug./Sep. 2011, pp. 1–9.

[7]. L. Xinchun, Shan Gao, J. Li, H. Lei and Y. Kang, "A new control strategy to balance neutral-point voltage in three-level NPC inverter," in *Proc.IEEE 8th Int.Conf Power Electron.ECCEAsia*, May/Jun. 2011, pp. 2593–2597.

[8]. J. Rodriguez, S. Bernet, P. K. Steimer and I. E. Lizama, "A survey on neutral-point-clamped inverters," *IEEE Trans. Ind. Electron.*, vol. 57, no. 7, pp. 2219–2230 Jul. 2010.

[9]. A. Lewicki, Z. Krzeminski, and H. Abu-Rub, "Space-vector pulsewidth modulation for three-level npc converter with the neutral point voltage control " *IEEE Trans. Ind. Electron.*, vol. 58, no. 11, pp. 5076–5086, Nov. 2011.

[10]. J. Pou, D. Boroyevich and R. Pindado,"Things of imbalances and nonlinear loads on the voltage balance of a neutral-point-clamped inverter,"*IEEE Tran. Power Electron*, vol. 20, no. 1, pp. 123–131, Jan. 2005.

[11]. Z. Huibin S. Jon Finney, A. Massoud, and B. W. Williams, "An SVM algorithm to balance the capacitor voltages of the three-level npc active power filter," *IEEE Trans. Power Electron.*, vol. 23, no. 6, pp. 2694–2702,Nov. 2008

[12]. J. Zaragoza, J. Pou, S. Ceballos E. Robles, C. Jaen, and M. Corbalan, "Voltage-balance compensator for a carrier-based modulation in the neutral-point-clamped converter," *IEEE Trans. Ind. Electron.*, vol. 56, no. 2, pp. 305–314, Feb. 2009.

[13]. W. Chenchen and L. Yongdong, "Analysis and calculation of zero sequence voltage considering neutral-point potential balancing in threelevel npc converters," *IEEE Trans. Ind. Electron.*, vol. 57, no. 7, pp. 2262–2271 Jul. 2010.

[14]. S.Busquets Monge, S. Somavilla, J. Bordonau, and D. Boroyevich,"Capacitor voltage balance for the neutral-point-clamped converter using the virtual space vector concept with optimized spectral performance," *IEEETrans. Power Electron.*, vol. 22, no. 4, pp. 1128–1135, Jul. 2007.

[15]. S. Busquets-Monge, J. Bordonau, D. Boroyevich, and S. Somavilla, "The nearest three virtual space vector PWM—A modulation for the comprehensive neutral-point balancing in the three-level NPC inverter," *IEEEPower Electron Lett.*, vol. 2, no. 1, pp. 11–15, Mar. 2004.